Structural Response of a Commercial Wind Turbine to Various Stopping Events

Jeffrey Bas[1], Jamie Smith[1], Rupp Carriveau[1]*, Shaohong Cheng[1], David S-K Ting[2] and Tim Newson[3]

[1]Department of Civil and Environmental Engineering, University of Windsor, Windsor, Ontario, Canada

[2]Department of Mechanical, Automotive, and Materials Engineering, University of Windsor, Windsor, Ontario, Canada

[3]Department of Civil and Environmental Engineering, University of Western Ontario, London, Ontario Canada

Submitted June 2, 2012, Revised September 13, 2012, Accepted September 21, 2012

ABSTRACT

Increases in forced curtailments at commercial wind farms have triggered a need to investigate turbine behaviour during stopping events. A 2.3 MW commercial horizontal axis wind turbine instrumented with a fiber Bragg grating strain array was subjected to the three most common types of stopping sequences performed by the turbine to measure the supporting tower's structural response. An overview of each considered stop type is included identifying their individual mechanical processes as well as their specific triggers. The along-wind and transverse strain measurements at varying elevations of the tower are presented and discussed. Distinguishable response characteristics for each stop type are identified at stop initiation, during rotor deceleration, and following event completion. Results obtained are subsequently compared to the tower strain reactions as a result of typical power production as well as pure yawing of the nacelle. Furthermore, the strain signal has been subjected to a discrete wavelet transform identifying variations in the signal frequency content, triggered by the stopping events.

1. INTRODUCTION

With global wind energy market penetration expected to hit 16% of the global electricity market by 2020 [1], wind energy is quickly becoming a mainstream source of electricity. According to the Canadian Wind Energy Association, total Canadian wind energy output is projected to reach 55,000 MW by the year 2025 [2]. The province of Ontario is currently the Canadian leader in wind energy with privately-owned generators responsible for a current wind capacity of 1676.5 MW with another 508 MW of production expected to be online by the end of the first fiscal quarter of 2013 [3].

As wind production capacity has increased, operators have reported an increase in forced curtailment. Forced curtailment and the subsequent turbine stops' effects on the turbine tower have been a growing concern for many commercial wind farm operators. In regions of high wind energy market penetration power transmission is often impeded by a lack of transmission capacity [4]. When transformers experience a real-time loading that exceed their emergency rating for more than a set period of time, a trip signal is sent to the wind farm's collector feeder.

*Corresponding author, Email: e. rupp@uwindsor.ca

This is known as grid loss, and as a result, the turbines are shut down in an emergency stop sequence [5].

The general dynamic properties of horizontal axis wind turbine towers have been well established in the literature through efforts focused on structural analysis completed by means of finite element analysis [6-11] and those involving the in-situ monitoring of towers using accelerometers and/or strain gauges [12-14]. Works dealing with transient events occurring during normal turbine operation and their structural implications have mainly focused on singular events such as yawing of the nacelle [15, 16] or individual types of stopping events [16-22]. Efforts have been made to quantify the root bending moment experienced by turbine blades [22], the forces and fatigue loads experienced by gearboxes [20] and foundation moments in order to assess the potential of geotechnical failures [21] as a result of emergency stopping events. Tower response to an unidentified stop type was demonstrated by [17] for the purpose of verifying the function of a fiber Bragg grating based sensory array (similar to the system employed by this study). The effectiveness of a point tracking videogrammetry system used to measure turbine motion by capturing the response of a commercial sized tower to an emergency stop was demonstrated by [18]. While [19] mentions the occurrence and subsequent response of a tower during both a normal and emergency stop; the report was focused more on advanced turbine controls, thus a detailed analysis of the structural response was not included; however, it was mentioned that the emergency stop had a greater impact on the turbine structure.

This manuscript investigates the structural strain response of a commercial scale horizontal axis wind turbine to three distinct production stopping events; normal stops, manual stops, and emergency stops. The strain in the turbine tower was monitored by a fiber Bragg grating sensor system during each stopping event over the span of 3 separate days of experimentation. The resulting responses from each type of stop are presented, compared, and discussed.

1.1. Types of stops

The Siemens 2.3 MW MKII Turbine is variable speed turbine with a rotor speed range of 0 to 16 rpm. It uses a conventional gearbox and it can employ any one of five different stopping sequences to take the turbine out of production. For the purpose of this experiment three stops were considered: the emergency stop sequence, the manual stop sequence, and the normal stop sequence. The two other stops were not considered as they are initiated solely due to highly specific turbine faults and were ultimately determined to be similar to an emergency stop. In all types of stops, the two main mechanisms used to slow the rotor to a stop are blade pitch and a disc brake. For the farm under study, the average number of stops per month was determined to be roughly 11.

The least intensive stopping sequence used to take a turbine out of production is the normal stop sequence. This stop is implemented from within the tower using the turbine's handheld control module or can be initiated remotely through the installation's supervisory control and data acquisition (SCADA) system. When the sequence is commenced the blades begin to pitch out of the wind to a pre-set reference pitch of 81.7 degrees known as 'safepitch'. The generator power is reduced proportionally with rotor speed. After 40 seconds the emergency stop valves in the rotor hub are opened to ensure the blades are fully pitched out of the wind in a fully feathered position and not generating any significant lift. Subsequently, the hydraulics within the machine that control the blade pitch are set to stop mode ensuring the blades remain in the safepitch position. During this stop there is no mechanical braking applied to the turbine . The normal stop sequence is used when personnel enter the turbine tower for routine maintenance or inspection where the parking brake is not required to be engaged.

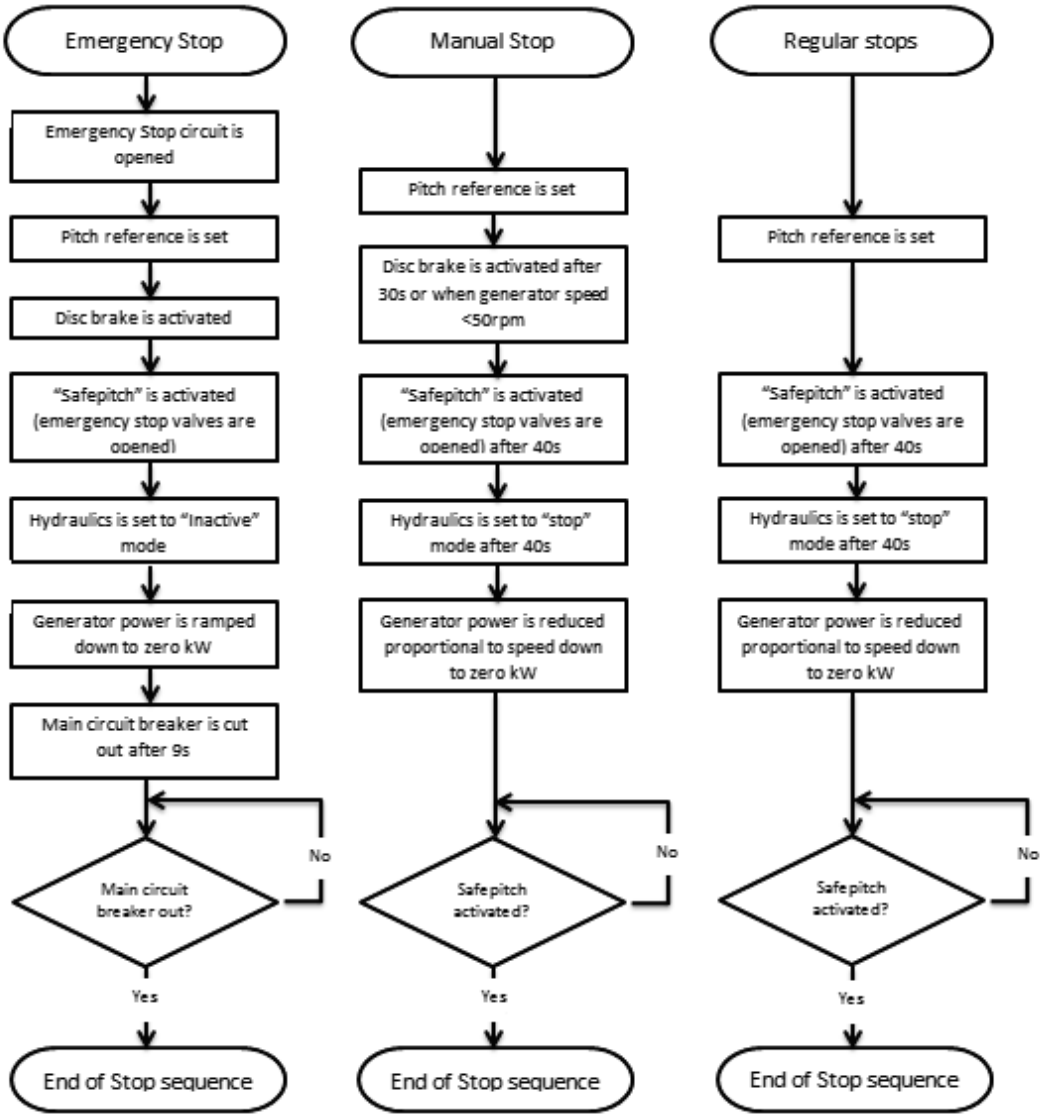

Figure 1: Flow chart depicting the three stop sequences tested.

The most commonly used stop is the manual stop. The manual stop is used anytime maintenance is conducted that requires the turbine rotor be held in a mechanically braked position. The stop sequence is identical to the normal stop sequence with the addition of the parking brake application. The parking brake, located on the high speed shaft is applied 30 seconds after the initial stop command, or when the generator speed becomes less than 50 rpm. The pressure is applied gradually to the brake disc until the rotor comes to a complete stop and is locked into a fixed position.

An emergency stop is the fastest stop the turbine can make and can be triggered by many events such as an emergency trip signal due to high grid loading [4, 5], a fault within the turbine control system, or manually triggered by depressing one of the emergency stop buttons located throughout the turbine. At the initiation of an emergency stop sequence, the demanded blade pitch is set to a pre-programmed pitch angle, and the emergency stop valves in the hub are activated to speed up the rate at which the blades pitch out of the wind into the safepitch position. The disk brake is activated immediately at initiation, applying full braking pressure.

The hydraulics in the nacelle are set to an inactive mode, the generator is quickly ramped down to 0 kW and the main breaker is cut out after 9 seconds.

2. EXPERIMENT

The fiber Bragg grating (FBG) strain sensor array utilized was capable of a 100 Hz data acquisition rate as presented in [15]. A total of 24 fiber optic strain gauges were affixed to the interior tower wall located 6 levels throughout the height of the wind turbine supporting tower with four gauges affixed at each level at due North, East, South and West positions. The tower is of steel plate construction with a height of 78.54 m, a maximum diameter of 4200 mm at its base, a minimum diameter of 2392 mm at the top and a wall thickness that varies along the height of the tower from 13 mm to 41 mm. Table 1 and Figure 2 summarize the heights of each strain gauge ring above the top of the tower foundation and show the positioning of the strain gauges around the inner tower wall, respectively, details are available in [15]. The tower was also subject to a recent inspection the results of which indicated that the tower was in good structural health.

Table 1: Vertical Location of Tower Strain Gauges.

Level	Vertical Height (m)
5	77.34
4	65.02
3	41.84
2	14.46
1	4.46
0	0

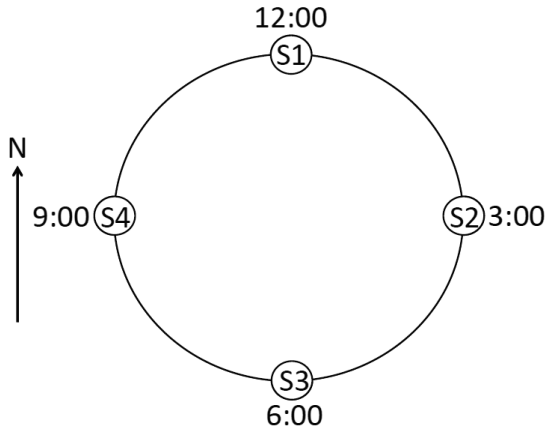

Figure 2: Typical sensor orientation.

Strain data was collected from the data acquisition system installed in the tower at 100 Hz and turbine operational data was collected at 0.2 Hz using the wind farm SCADA system. The turbine operational parameters recorded were: yaw angle, rotor rpm, blade pitch, active power, wind speed, ambient temperature and main bearing temperature.

The experiment was carried out over three separate days of good wind production with rotor speeds at the maximum steady operating speed of 16 rpm. In total 9 normal stops, 8 manual stops

and 2 emergency stops were performed. All normal and manual stops were initiated from within the tower using the handheld tower control module; the emergency stops were initiated by hitting the emergency stop button in the base of the tower. Only two emergency stops were conducted due to the operator's concerns over undue damage to mechanical components within the nacelle.

3. RESULTS

A summary of the characteristics of the three different stop types, as recorded by the tower's SCADA data log, is presented in Table 2 below. It can be seen that the normal stop sequence is the least abrupt among the 3 stops studied, with an average duration of 35 seconds and an average rotor deceleration rate of 0.46 rpm/sec. Given that the normal stop does not apply a parking brake to the rotor, the sequence was deemed complete when the rotor rpm is first registered as 0 on the SCADA recording. Due to the resolution limitations of the system, a zero reading corresponds to a rotor speed of less than 0.5 rpm.

Table 2: Stop Summaries.

Stop Type	Number of Tests	Duration (sec)	Deceleration (rpm/sec)	Average rpm Immediately	rpm at Application of Disc Brake Before Stop
Normal	9	35	0.46	16	—
Manual	8	31.9	0.50	16	1
Emergency	2	17.5	0.91	16	16

The manual stops averaged a duration of 31.9 seconds with a deceleration rate of 0.50 rpm/sec. The parking brake was applied after 30 seconds from the initial stop command, and at this time the rotor rpm was 1 during every stop sequence tested. Upon comparing the regular stopping sequence and the manual stopping sequence it was concluded that both stops were very similar in duration due to the primary braking mechanism being aerodynamic. The parking brake is applied only to lock the rotor to keep it from idling. The emergency stop was the most abrupt, recording an average stop time of 17.5 seconds with a deceleration rate of 0.91 rpm/sec. This confirms the effect that the mechanical disc brake and the increase in blade pitch speed have on the deceleration rate - essentially cutting the stop duration in half.

Figures 3 and 4 shows the results from tests conducted on September 15th 2011, displaying the strain recorded at the North strain gauge at Level 0, zero meters above the top of the tower's foundation. The wind was blowing at a mean speed of 8.5 m/s from the North, aligned with the North and South strain gauges, producing nearly pure windward strain response measurements of the North face. These figures also shows the blade pitch recorded during the experiment. It is important to note that the strain measured during the experiment is not absolute, but a relative strain with respect to the initial strain reading of the experiment. For the sake of demonstration and ease of interpretation, the zero axis was shifted to the average strain measurement corresponding to the stopped turbine. There was a slight error in the alignment of the timestamps on both the strain response dataset and the tower SCADA recordings; as a result both data sets were manually synchronized by identifying the beginning of the stops in the SCADA dataset characterized by the pitching of the blades to the pre-programmed pitch of 81.8°.

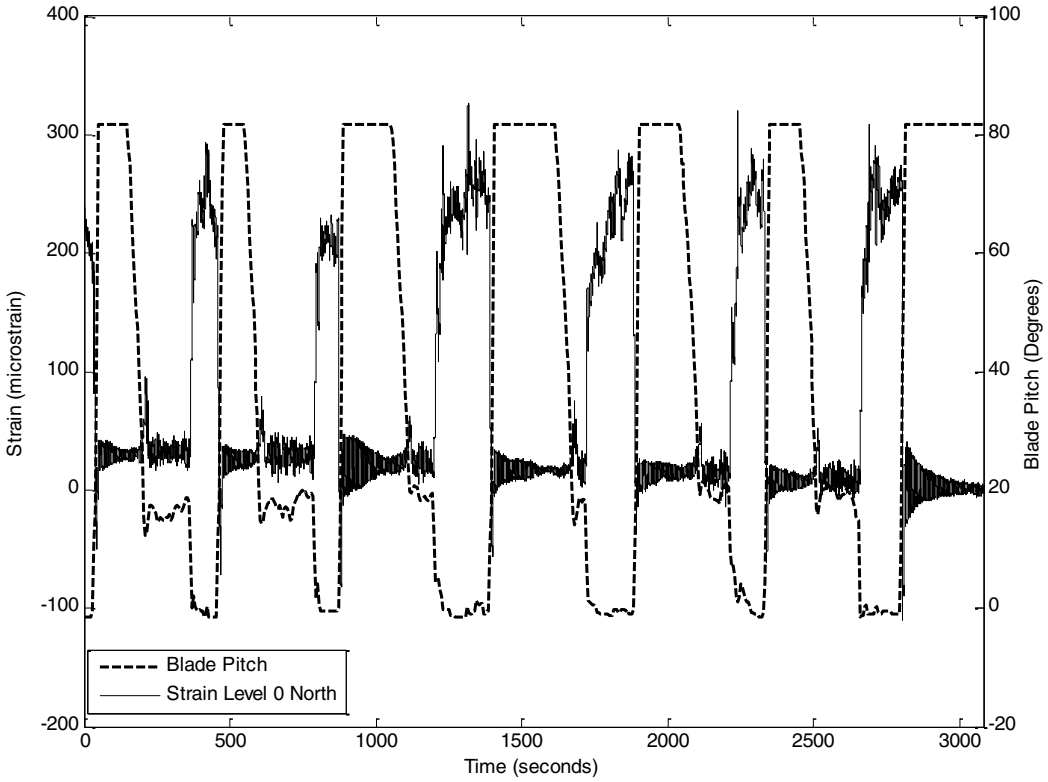

Figure 3: Strain and blade pitch vs. time during the test on September 15th, 2011.

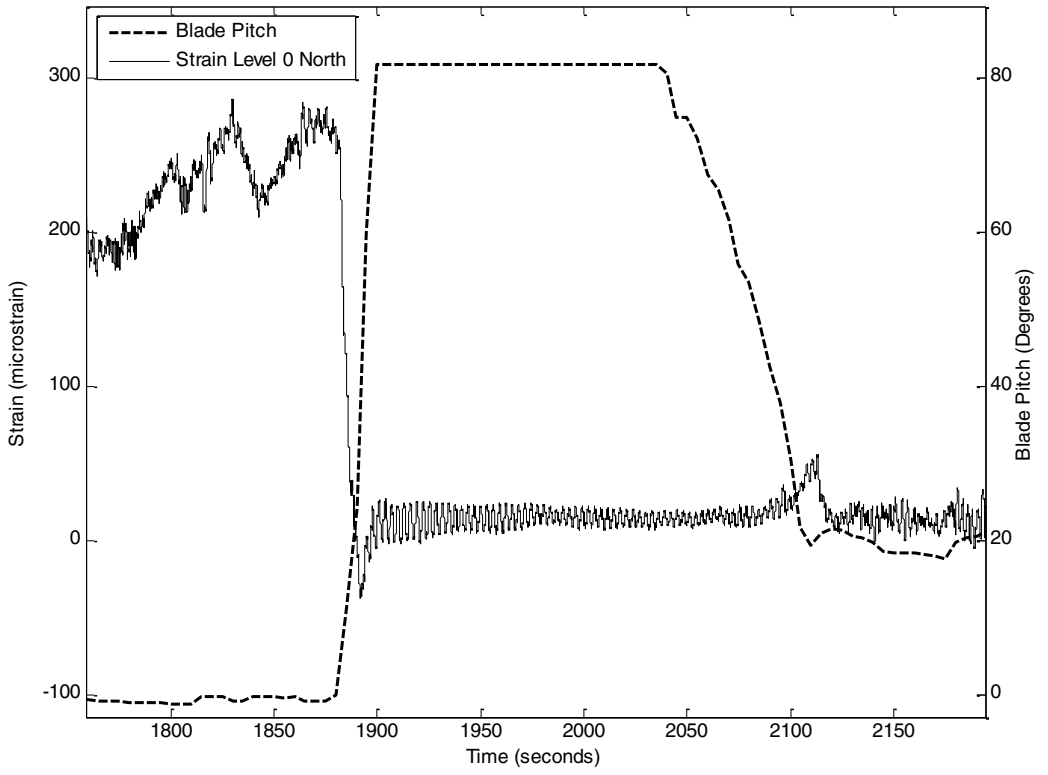

Figure 4: Detailed view of strain and blade pitch vs. time during an individual stop on September 15th,2011

The experiment depicted in Figure 3, consisted of 7 stops in total; the first three stops were normal stops, starting at the 21, 446, and 861 second marks, the next three stops beginning at the 1376, 1872 and 2316 second marks of the experiment were manual stops and the very last stop during the experiment was an emergency stop beginning at the 2786 second mark. The more sporadic regions of higher strain preceding the stops are periods of normal power production.

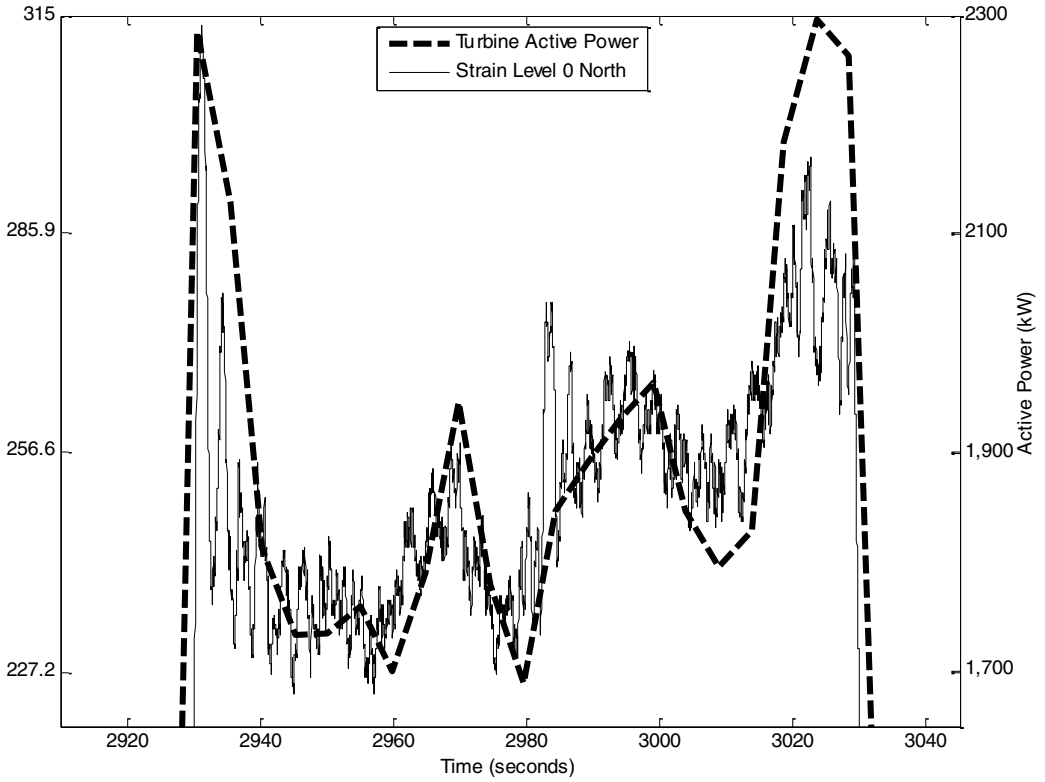

Figure 5: Strain and active power vs. time January 19th, 2012.

The major loading change on the tower during a stopping event coincides with the pitching of the blades out of the wind, and confirms that the motion of the tower is strongly coupled with the blades as they transfer the axial forces that are a result of power extraction [23]. This is demonstrated in Figure 5 that shows the along-wind strain response of the tower at Level 0 and the active power being produced by the turbine's generator during normal power production between two stops, noting the correlation between the two. This great reduction in load transferred to the top of the tower through the hub assembly is clearly evident in all types of stops considered in this study. Another commonality in the along-wind response between the three stops considered is a strain peak present in the final moments of blade pitch while the rotor is in the process of coming to a rest. This negative peak is a result of negative thrust due to a momentary negative angle of attack [20, 24]. The magnitudes of the negative strain peaks are seen to be related to the different type of stops used. Taking the normal and manual stops as a baseline, the emergency stops experienced a negative strain peak of 189% greater than the negative strain peak of the normal stops. It can be seen in Figure 6 that the tower displays a decaying response similar to that of a structure in free vibration.

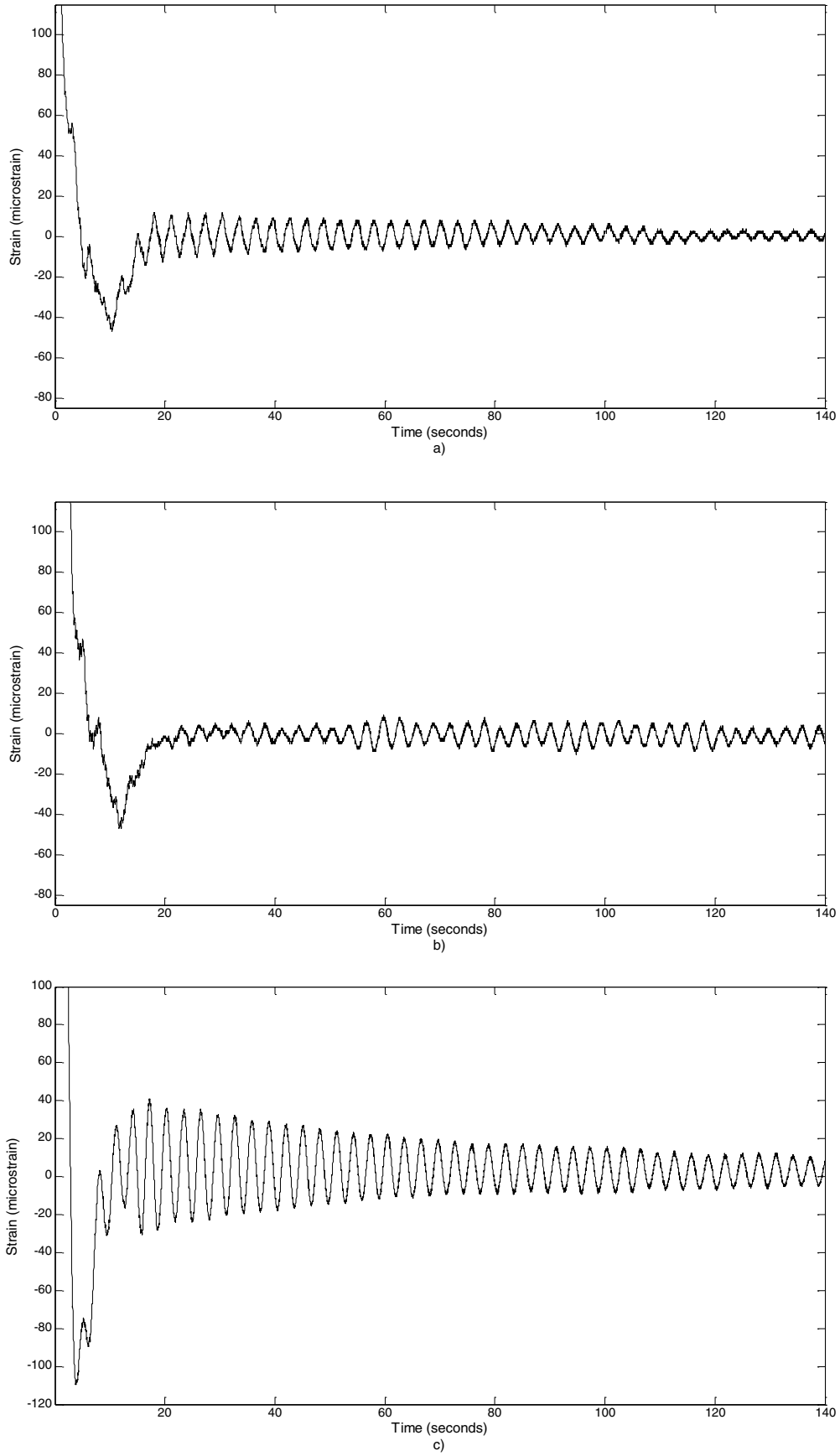

Figure 6: Raw strain response from typical: a) regular stop, b) manual stop, c) emergency stop.

Upon closer inspection of the strain response for each of the three different stop types in Figure 6, subtle differences are present as the tower settles. Both the regular and manual stops (Figure 6 (a) & (b)) demonstrate very similar behaviour following the negative strain peak. However, the tower's response following the manual stop seems to be more random in nature. This trend is observed in all regular and manual stop events tested, and it is supposed that this is due to the fixed condition of the rotor to the tower while the parking brake is engaged. As opposed to being in a slow idle situation where any out-of-plane aerodynamic forces acting on the blades can be transmitted into rotation, as is the case with the post-stop condition of the regular stop; the parking brake causes all out-of-plane forces to be transmitted into the tower resulting in a subsequent response. The emergency stop response (Figure 6(c)) is more dramatic than the regular and manual stops, beginning with the negative strain peak and ensuing free vibration. Strain amplitudes nearly double those of the aforementioned stop types are observed, and are thought to be the result of the abruptness of the emergency stop. That said, after the tower's periodic response begins to settle to amplitudes similar to the regular stop, the tower displays the same random tower response to the prior mentioned out-of-plane aerodynamic forces.

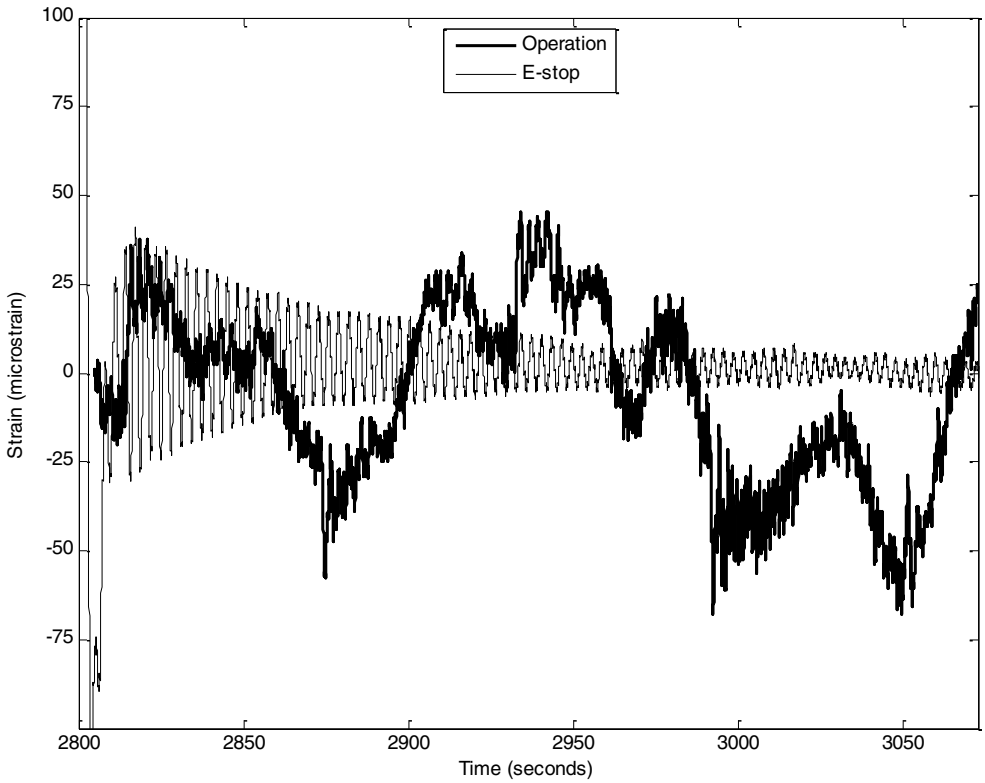

Figure 7: Comparison of emergency stop strain response and to strain response during typical turbine operation for strain gauge located at Level 0 North.

The along-wind strain response of the tower during an emergency stop was compared to that of the tower during normal power production before the commencement of the stop experiment (Figure 7 shown above). The strain during production's datum was shifted for ease of interpretation to establish the difference in magnitude of strain variation during a stopping event versus the tower strain response during normal operation. Wind speeds during the recording

period of the operational data were 7.8 m/s with a standard deviation of 1.0 m/s; these wind speeds are representative of the region's mean wind speeds of 8.0 m/s, as obtained from the Canadian Wind Energy Atlas [25]. The recordings took place within an hour of one another. Although operational response can change dramatically depending on incoming wind flow, it is worth noting that the variance and range of values in tower strain response to normal operating conditions is greater than that of the tower settling to rest following the initial period of negative thrust in an emergency stop.

The strain response at the top of the wind turbine tower perpendicular to the wind (in the rotor plane) was also examined. Due to the uppermost strain gauges' proximity to the tower-nacelle interface, the gauges are able to detect the strain response of the tower resulting from the application of the parking brake. The strain measured at the top of the tower transverse to the wind direction reveals unique signatures for each of the stops considered. Beginning with the normal stop (Figure 8(a)), the response demonstrates the settling of the tower to a near steady-state strain level after the turbine slowed to idle. The transverse strain signature of the manual stop (Figure 8(b)) during the initial tower reaction closely mirrors that of the regular stop until the rotor rpm reaches 1 where the parking brake is engaged to slow the rotor to a complete stop. At the instant of brake application there is a clear rise in strain; likely the result of torque induced in the tower as consequence of mechanically braking the rotor. After the rotor rotation has ceased, the strain response seems more active and random compared to the strain response of the tower following the normal stop. This is due to the rigid condition created when the parking brake is applied, forcing the loads due to the interactions of the rotor assembly and the wind to be transferred into the tower. The transverse strain at the top of the tower during the emergency (Figure 8(c)) stopping sequence demonstrates a much greater initial response when compared to the previous stopping events. As an emergency stop sequence is initiated the disc brake is immediately engaged; this results in a dual stage torque-induced strain peak with one peak arriving almost immediately after brake application and another smaller subsequent strain peak when the rotor comes to a complete stop. The tower response afterwards resembles that of the regular stop as it ends up in the same parked condition. As discernible as these strain responses to each stop type are, it has been shown that the magnitude of the strain variation at the top of the tower due to the regularly shifting eccentric load produced by the self-weight of the nacelle and rotor assembly is more than 2.5 times greater than the strain range during an emergency stop [15].

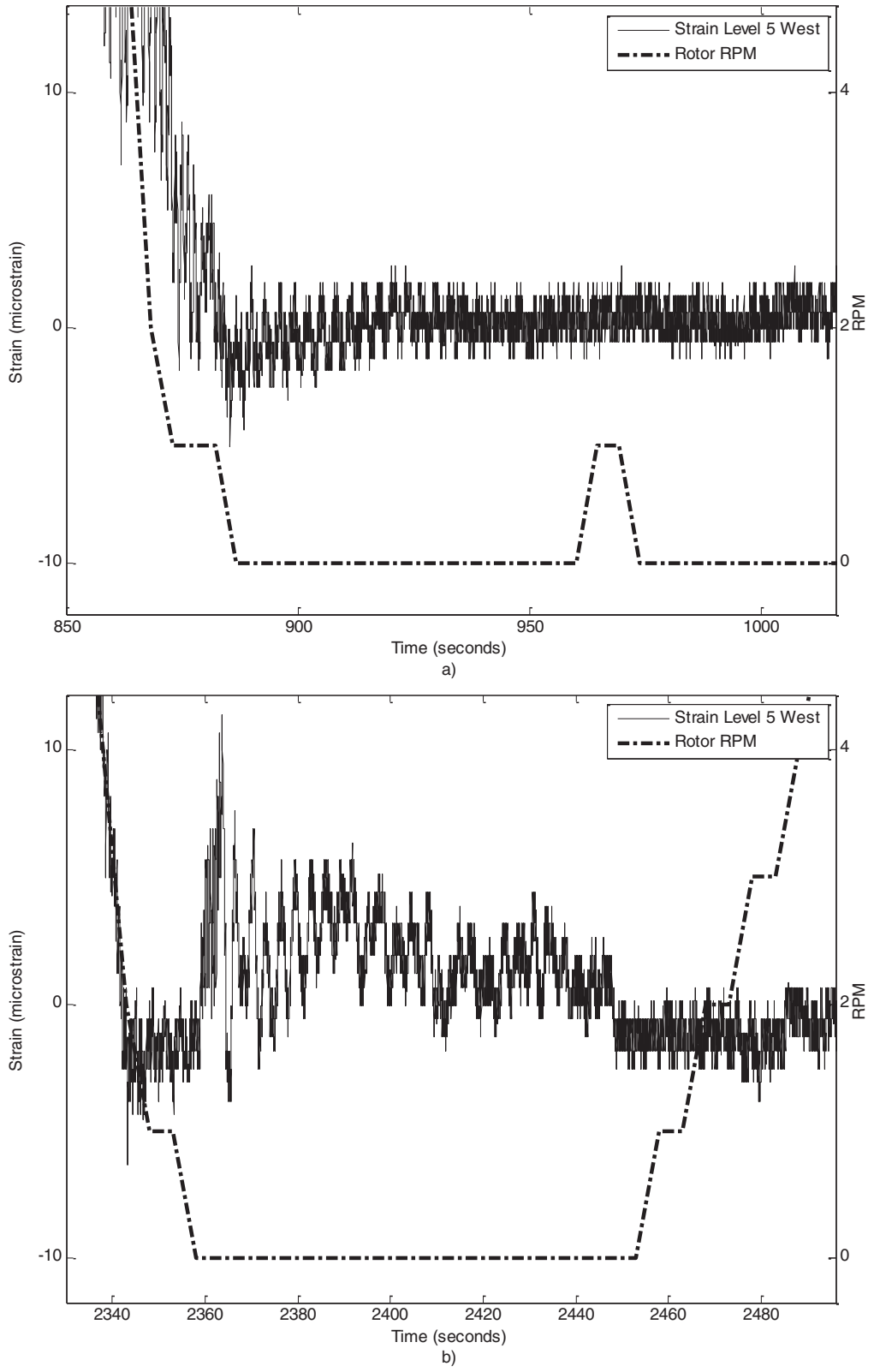

Figure 8: Transverse strain response at the top of the tower for a) regular stop, b) manual stop and c) emergency stopping events.

3.1. Wavelet Analysis

Given the variability in environmental conditions and turbine operational parameters over the three testing days, wavelet analysis was employed to provide further insight into the nature of the tower strain response to turbine stopping sequences. Wavelet analyses can determine the frequency content of a signal using functions derived from the translation and dilation of a mother wavelet [26, 27]. Unlike traditional Fourier analysis, which determines a signal's overall frequency content, the use of wavelets permits the study of variations in a signal's frequency content over time. Using dyadic scales, the discrete wavelet transform (DWT) discretizes and decomposes the signal into decomposition levels related to wavelet scale [27].

In the past, Daubachies 6th order wavelet has been applied in vibration analysis of the 2.3 MW wind turbine under study. Earlier work in [16, 28] analyzed turbine vibration response to start up, steady state operation, yaw motion, and stopping events. Daubachies 6th order wavelet has also shown previous success in fault detection in a rotor [29], and subsequently was selected as the mother wavelet for analysis.

The pseudo frequency corresponding to each decomposition level can be found using the following equation [30]:

$$F_a = \frac{F_c}{a \cdot \Delta} \tag{1}$$

where F_a is the pseudo frequency, F_c is the centre frequency of the wavelet ($\cong$ 0.7273 Hz for Daubachies 6th order wavelet), a is the wavelet scale, and Δ is the sampling period (0.01 s for the strain data acquisition system in place). An 11-level DWT will be used, given the unnecessarily low pseudo frequency associated with a 12^{th} decomposition level. The pseudo frequencies for each level are outlined in Table 3.

Table 3: Pseudo Frequencies Associated With Individual Decomposition Levels.

Level	Scale	Pseudo Frequency (Hz)
11	2048	0.0355
10	1024	0.0710
9	512	0.1420
8	256	0.284
7	128	0.568
6	64	1.136
5	32	2.27
4	16	4.55
3	8	9.09
2	4	18.18
1	2	36.4

3.2. Analysis of Two Testing Periods

DWT analysis was conducted on the two experimental periods in which an emergency stop was performed. The purpose of these analyses was to identify general similarities and briefly characterize the variations in frequency content of tower strain response for the three types of stops surveyed in this paper.

The DWT coefficient plots for the North strain gauge at Level 0 for the set of stops conducted on September 15th and November 4th are shown in Figure 9 and Figure 10, respectively. The darker shades indicate higher coefficient values, and the section of each plot coinciding with the initiation of the emergency stop sequence is circled. Given the poor signal-to-noise ratio the sensor array exhibits at higher frequency levels, the strain signal has been de-noised for the purpose of these analyses, which has eliminated the signal component at the first three decomposition levels. On September 15th, the wind blew from the North, generating a nearly pure windward response in the North strain gauge. Each of the 7 stop sequences conducted on this day are indicated by high signal energy at the 11th decomposition level in Figure 9, which is the effect of the immediate and drastic change in tower strain levels following the initiation of the stopping sequence as the turbine transitions out of production, as has been shown in Figure 3. The portion of the strain signal generated by the initiation of the emergency stop sequence also demonstrates high signal energies in the 8th, 9th, and 10th decomposition levels. The East and West gauges were positioned out-of-line with the predominant wind direction during the testing period on September 15th, and therefore show weaker and less consistent signal energy for manual and regular stops. However, the effect of the emergency stop remained evident with high signal energy in levels 8 through 11.

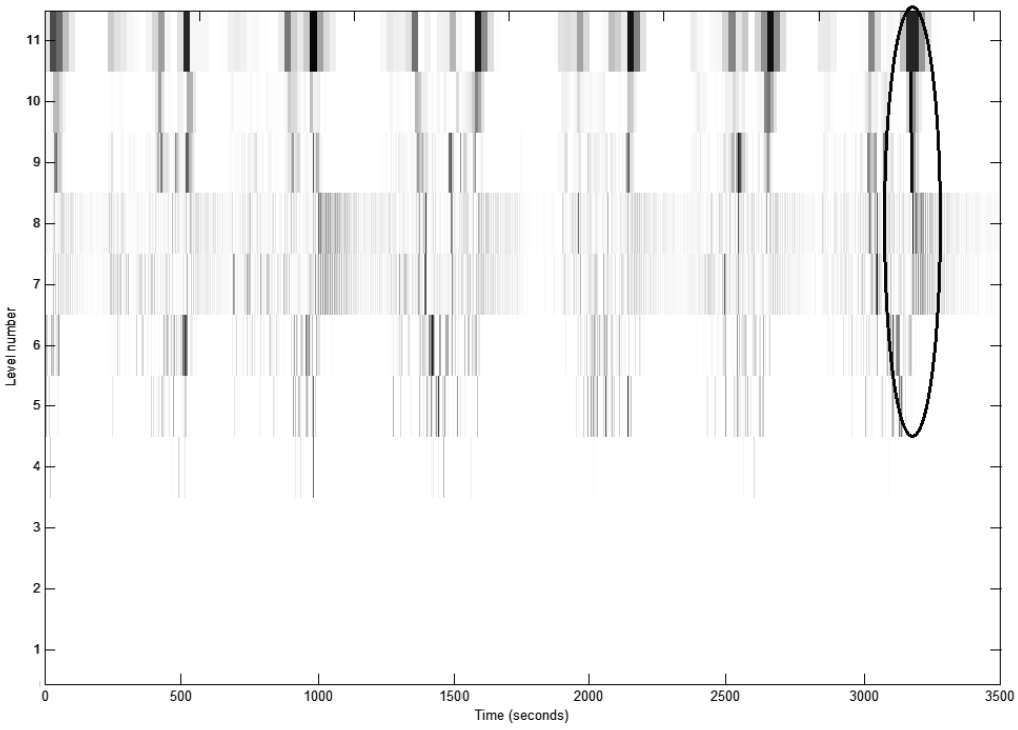

Figure 9: DWT coefficient plot for North gauge on September 15th.

On November 4th, the wind blew from the Northeast. As a result, the appearance of high signal energy at the 11th decomposition level for each of the 5 stop sequences is less consistent in Figure 10. However, the emergency stop sequence continues to demonstrate high signal energy in levels 8 through 11. The DWT analyses conducted for the two testing periods suggest a wider frequency range in the immediate strain response for emergency stops, which is less dependent on the relative position of the rotor than for regular and manual stops. It is speculated that this

behaviour is resulting from the impulse load generated by the early activation of the disc brake in an emergency stop sequence while the rotational speed of the rotor is still high.

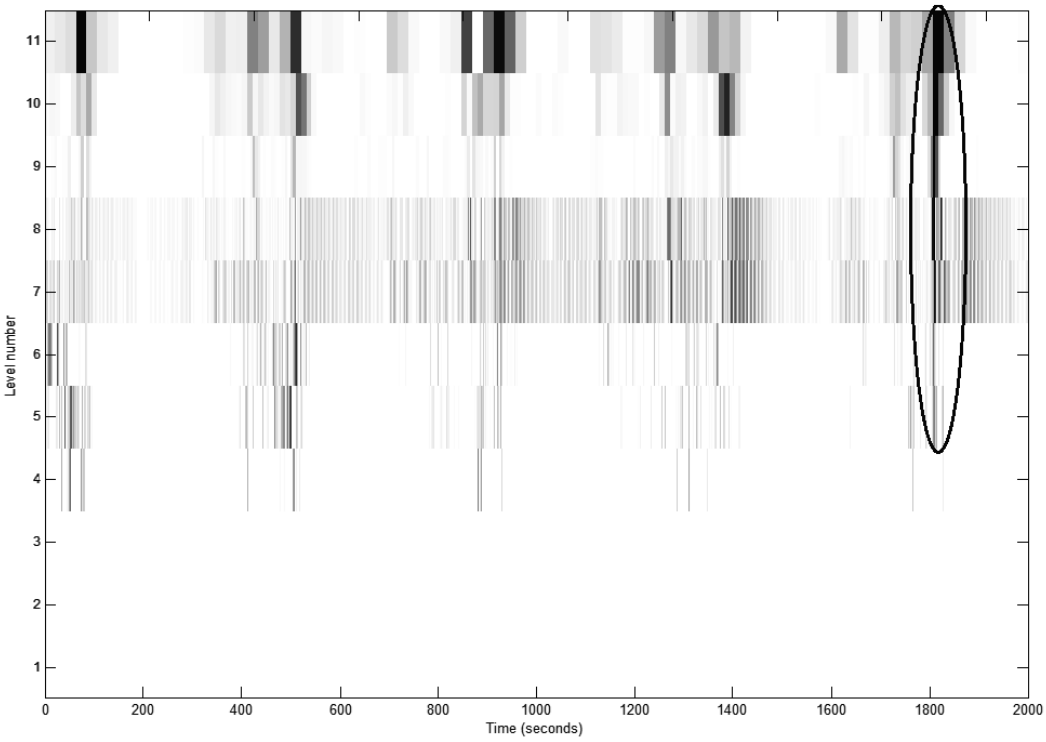

Figure 10: DWT coefficient plot for North gauge on November 4th.

An isolated view of the DWT coefficient plot and de-noised strain signal for the emergency stop conducted on September 15th is shown in Figure 11. High signal energies are seen at the 7th and 8th decomposition levels, which slowly dissipate as the tower enters free vibration following the completion of the stopping sequence. This pattern is similarly exhibited following the manual and regular stops, and corroborates with the findings in [16] where low frequency activity in the vibration signal was observed to persist following manual stopping sequences. The frequency window spanned by decomposition levels 7 and 8 (0.1420 – 0.568 Hz) occupy the range of expected first natural frequencies for turbines of this design and magnitude [21, 31]. The identification of the first mode response as well as the frequency of stops experienced by a typical turbine in this wind farm could potentially contribute to a basis of a response-founded structural health monitoring scheme.

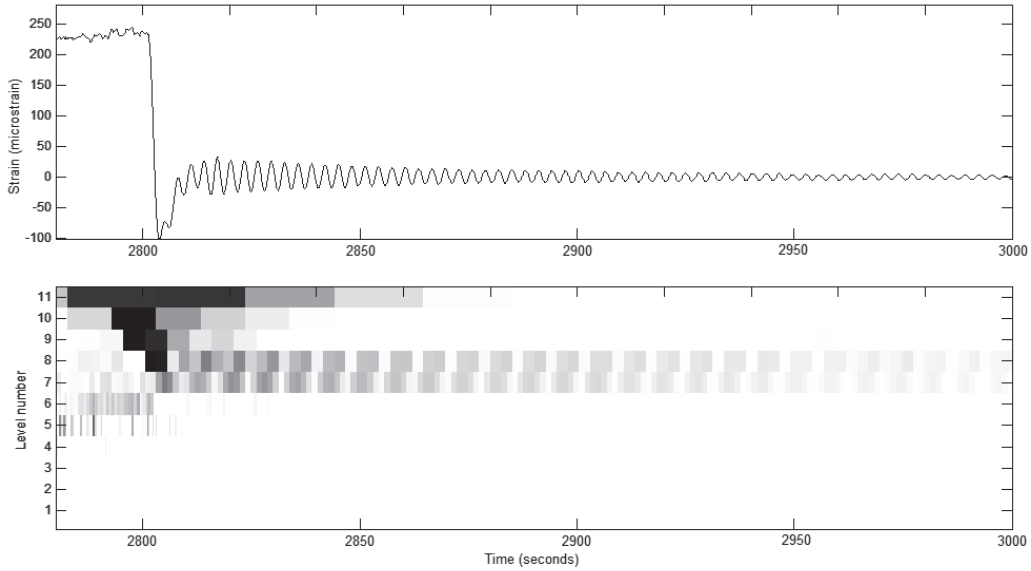

Figure 11: Isolated DWT plot and strain signal for North gauge during emergency stop on September 15th.

4. CONCLUSIONS

The strain response of a 2.3 MW operational commercial wind turbine tower was measured and analyzed during three different rotor braking events; regular, manual, and emergency. The following conclusions are made.

- The major structural response of the tower in all three stopping cases was determined to be caused by the aerodynamic unloading of the tower, followed by a period of negative thrust that occurred during the first moments of each stop. The subsequent tower response resembled a state of free vibration.
- The tower showed a very similar strain response to both the regular and manual stop types, the only differences were caused by the application of the rotor parking brake at the end of each stop sequence.
- Comparing the along-wind response of the tower during an emergency stopping event to the response of both the regular and manual stops, the tower showed a much greater initial strain response during an emergency stop event. However, this initial response is transient in nature and it eventually settles to that of the regular stop.
- In the transverse strain direction, the response during an emergency stop measured at the uppermost section of the tower demonstrated two strain peaks; the first peak corresponding to the initial application of the brake and the second occurred as the rotor reached 0 rpm.
- Overall the strain response due to all stopping events have not proven to be more severe than those caused by the operational condition the tower undergoes on a daily basis whether it be normal power production, nacelle yawing, or even responses to large wind variations.
- Among the lower frequency levels capable of being measured by the sensor array with an acceptable signal-to-noise ratio, wavelet analyses showed that the immediate tower structural response to emergency stops demonstrated a wider frequency range of high signal energy when compared to the response of manual and regular stops, and that the effect of the emergency stops persisted regardless of relative rotor position.

- Wavelet analysis demonstrated high signal energy in the frequency window between 0.1420 – 0.568 Hz during the free vibration of the tower following each stopping sequence.

ACKNOWLEDGEMENTS

The authors would like to acknowledge the generous support of their industrial partner, particularly, the keen insights and advice from Michael Cookson, JJ Davis, Paul Dawson, and Jason Stoner.

REFERENCES

[1] Blanco, M. I., The Economics of Wind Energy, *Renewable & Sustainable Energy Reviews*, 2009, 13(6-7), 1372-1382.

[2] Canadian Wind Energy Association, WindVision 2025: Powering Canada's Future, 2008.

[3] Independent Electricity System Operator, Wind Power in Ontario, March 30 2012. http://www.ieso.ca/imoweb/marketdata/windpower.asp

[4] Burke, D. J. and O'Malley, M. J., Transmission Connected Wind Curtailment with Increasing Wind Capacity Connection, 2009 IEEE Power & Energy Society General Meeting (PES), *IEEE*, New York, 2009.

[5] Acharya, N., Liu, C.-C. and Djukanovic, M. B., Wind Generation Curtailment to Relieve Line Overload in an On-Line Environment, *European Transactions on Electrical Power*, 2009, 19(6), 854-868.

[6] Xu, Y., Sun, W. and Zhou, J., Static and Dynamic Analysis of Wind Turbine Tower Structure, *Advanced Materials Research* (vol. 33-37), Trans Tech Publications, Germany, 2008, 1169-1174.

[7] Wang, L. and Dong, X., Influence of Earthquake Directions on Wind Turbine Tower Under Seismic Action, *Advanced Materials Research* (vol. 243-249), Trans Tech Publications, Germany, 3883-3888.

[8] Binh, L. V., Ishihara, T., Phuc, P. V. and Fujino, Y., A Peak Factor for Non-Gaussian Response Analysis of Wind Turbine Tower, *Journal of Wind Engineering and Industrial Aerodynamics*, 2008, 96(10-11), 2217-2227.

[9] Lavassas, I., Nikolaidis, G., Zervas, P., Efthimiou, E., Doudoumis, I. N. and Baniotopoulus, C. C., Analysis and Design of the Prototype of a Steel 1-MW Wind Turbine Tower, *Engineering Structures*, 2003, 25(8), 1097-1106.

[10] Chen, X.-B., Li, J. and Chen, J.-Y., Wind-Induced Response Analysis of a Wind Turbine Tower Including the Blade-Tower Coupling Effect, *Journal of Zhejiang University: Science A*, 2009, 10(11), 1573-1580.

[11] Murtagh, P. J., Basu, B. and Broderick, B. M., Along-Wind Response of a Wind Turbine Tower with Blade Coupling Subjected to Rotationally Sampled Wind Loading, *Engineering Structures*, 2005, 27(8), 1209-1219.

[12] Pollino, M. C. and Huckelbridge, A. A., Jr., Initial Observations from Monitoring the In-Situ Performance of a Community-Scale Wind Turbine Support Structure, *IEEE 2011 EnergyTech*, IEEE, New Jersey, 2011.

[13] Molinari, M., Pozzi, M., Zonta, D. and Battisti, L., In-Field Testing of a Steel Wind Turbine Tower, *Conference Proceedings of the Society for Experimental Mechanics Series (vol. 1)*, Springer New York, New York, 2011, 103-112.

[14] Swartz, R. A., Lynch, J. P., Zerbst, S., Sweetman, B. and Rolfes, R., Structural Monitoring of Wind Turbines Using Wireless Sensor Networks, *Smart Structures and Systems*, 2010, 6(3), 183-196.

[15] Bas, J., Carriveau, R., Cheng, S., and Newson, T., Strain Response of a Wind Turbine Tower as a Function of Nacelle Orientation, *BIONATURE 2012: The Third International Conference on Bioenvironment, Biodiversity and Renewable Energies*, IARIA, 2012, 12-18.

[16] Bassett, K., Carriveau, R. and Ting, D. S.-K., Vibration Response of a 2.3 MW Wind Turbine to Yaw Motion and Shut Down Events, *Wind Energy*, 2011, 14(8), 939-952.

[17] Bang, H.-J., Jang, M. and Shin, H., Structural Health Monitoring of Wind Turbines Using Fiber Bragg Grating Based Sensing System, *Proceedings of SPIE – The International Society for Optical Engineering* (vol. 7981), SPIE, United States, 2011.

[18] Paulsen, U. S., Erne, O., Moeller, T., Sanow, G. and Schmidt, T., Wind Turbine Operational and Emergency Stop Measurements Using Point Tracking Videogrammetry, *Society for Experimental Mechanics – SEM Annual Conference and Exposition on Experimental and Applied Mechanics 2009* (vol. 2), Society for Experimental Mechanics, Connecticut, 2009, 1128-1137.

[19] Johnson, K., Fingersh, L. J. and Wright, A., Controls Advanced Research Turbine: Lessons Learned During Advanced Controls Testing, *NREL/TP-500-38130*, National Renewable Energy Laboratory, Colorado, 2005.

[20] Heege, A., Radovcic, Y. and Bertran, J., Fatigue Load Computation of Wind Turbine Gearboxes by Coupled Structural, Mechanism and Aerodynamic Analysis, *DEWI Magazin*, 2006, 28, 61-68.

[21] Branca, B. and Ben-Hassine, J., Dynamic Analysis of a Wind Turbine and Foundation to Assess Liquefaction Potential of Bearing Soils, *Proceedings of the 2009 Structures Congress – Don't Mess with Structural Engineers: Expanding Our Role*, ASCE, Virginia, 2009, 2107-2118.

[22] Ahlström, A., Emergency Stop Simulation Using a Finite Element Model Developed for Large Blade Deflections, *Wind Energy*, 2006, 9(3), 193-210.

[23] Harrison, R., Hau, E. and Snel, H., *Large Wind Turbines: Design and Economics*, John Wiley and Sons Ltd., New York, 2000.

[24] Hau, E., *Wind Turbines: Fundamentals, Technologies, Application, Economics*, Springer, Munich, 2000.

[25] Environment Canada, Canadian Wind Energy Atlas: Maps, March 22 2012. http://www.windatlas.ca/en/maps.php

[26] Sweldens, W., The Lifting Scheme: A Construction of Second Generation Wavelets, *SIAM Journal on Mathematics Analysis*, 1997, 29(2), 511-546.

[27] Luo, G. Y., Osypiw, D. and Irle, M., On-Line Vibration Analysis with Fast Continuous Wavelet Algorithm for Condition Monitoring of Bearing, *Journal of Vibration and Control*, 2003, 9(8), 931-947.

[28] Bassett, K., Carriveau, R. and Ting, D. S.-K., Vibration Analysis of 2.3 MW Wind Turbine Operation Using the Discrete Wavelet Transform, *Wind Engineering*, 2010, 34(4), 375-388.

[29] Adewusi, S. A. and Al-Bedoor, B. O., Wavelet Analysis of Vibration Signals of an Overhang Rotor with a Propagating Transverse Crack, *Journal of Sound and Vibration*, 2001, 246(5), 777-793.

[30] Abry, P., *Ondelettes et turbulence. Multirésolutions, algorithmes de décomposition, invariance d'échelles*, Diderot Editeur, Paris, 1997.

[31] Bonnett, D., Wind Turbine Foundations- Loading, Dynamics and Design, *Structural Engineer*, 2005, 83(3), 41-45.